

An Improved Turbo Decoding Scheme for Impulsive Channel

Savitha H. M., Muralidhar Kulkarni

Department of Electronics and Communication Engineering,
National Institute of Technology Karnataka, Surathkal, Karnataka, India
e-mail: savithahm@yahoo.com, mkuldce@gmail.com

Abstract— This paper proposes a novel turbo decoding scheme for additive white class A noise (AWAN) channel. It compares the performance of turbo coded systems with Quadrature Phase Shift Keying (QPSK) and 16-Quadrature Amplitude Modulation (16-QAM) on AWAN channel with two different channel values—one computed as per additive white Gaussian noise (AWGN) channel conditions and the other as per AWAN channel conditions. The results show that the use of appropriate channel value in turbo decoding helps to combat the impulsive noise more effectively. Also, the Bit error rate (BER) performance of the proposed model for AWAN channel is compared with that of AWGN channel. It is observed that they exhibit comparable BER performance.

Keywords- 16-QAM, Turbo code, Bit error rate, AWAN channel

I. INTRODUCTION

Turbo codes were initially introduced by Berrou, Glavieux and Thitimajshima. It uses two or more concatenated or parallel codes on different interleaved versions of the original data. The decoders exchange soft decisions rather than hard decisions so that best results are achieved. A typical turbo encoder uses parallel concatenated convolutional codes (PCCC) in which data bits are coded by two or more recursive systematic convolutional (RSC) coders, each with input as interleaved versions of data. In a turbo system with two component decoders, the decisions from one component decoder are passed as input to another decoder and this process is iteratively done for several times to get more reliable decisions. The high error correction power of turbo code originates from the random interleaving at the encoder and iterative decoding using extrinsic information at the decoder [1]-[3].

Power line communication (PLC) is an innovative idea of transmitting the telecommunication signal through the public power network. What makes this new technology more appealing is that it utilizes the existing infrastructure and there is no need for new wires. One of the challenges in PLC technology is to combat the electromagnetic noise on power line channels, having impulsive characteristics, introduced by the electrical appliances. Middleton's Class A noise model [4], [5] for non-Gaussian noise channels is used for modeling of man-made impulsive noise channels, for example, wireless channels, power line channels, etc.

The above mentioned noise model corresponds to an independent and identically distributed (i.i.d.) discrete-time random process whose probability density function (PDF) is

an infinite weighted sum of Gaussian densities, with decreasing weights and increasing variance for the Gaussian densities [5].

II. TURBO CODED SYSTEMS

A. Turbo Encoder

The encoder of PCCC turbo system with two RSC coders is shown in Fig.1. The binary input data sequence is represented by $d_k = (d_1, \dots, d_N)$. The input sequence is passed into the input of the first RSC coder, ENC1 that generates a coded bit stream, x_k^{p1} . For the second RSC coder ENC2, the data sequence is interleaved using random interleaver in which the bits are output in a pseudo-random manner. The interleaved data sequence is passed to ENC2, and a second coded bit stream, x_k^{p2} is generated. The output code sequence of the turbo encoder is a multiplexed (and possibly punctured) stream consisting of systematic code bits x_k^s along with the parity bits of first and second encoders, x_k^{p1} and x_k^{p2} [6].

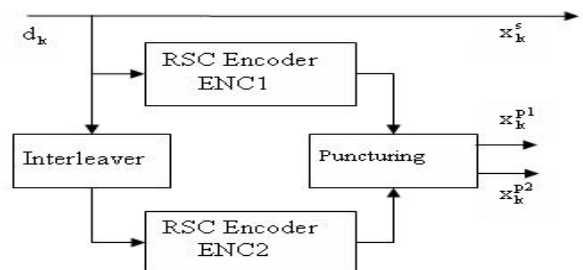


Figure 1. Turbo Encoder

B. Turbo Decoder

The Turbo decoder consists of two component decoders – DEC1 to decode sequences from ENC1, and DEC2 to decode sequences from ENC2 as shown in Fig. 2. It takes a sequence of received code values, $r_k = \{y_k^s, y_k^p\}$. Both the decoders are Maximum A Posteriori (MAP) decoders. DEC1 takes y_k^s , the systematic values of the received sequence along with y_k^{p1} which is the received sequence parity values belonging to the

first encoder ENC1. Sequence of soft estimates $L_{e1}(\hat{d}_k)$ of the transmitted data d_k that are available at the output of DEC1, are interleaved and passed to the second decoder DEC2 as a priori information. The same interleavers are used at both encoder and decoder. The three inputs to DEC2 are as follows: interleaved version of the systematic received values y_k^s , sequence of received parity values from the second encoder y_k^{p2} and interleaved version of the soft estimates $L_{e1}(\hat{d}_k)$. The a priori information for first decoder, $L_{e2}(\hat{d}_k)$ is obtained from de-interleaving the soft estimates of DEC2. This procedure is repeated in an iterative manner for required number of iterations, and the final a posteriori output of the second decoder is de-interleaved to get the log likelihood representation of the estimate of d_k . Larger negative values of the likelihood ratio $\Lambda(\hat{d}_k)$ represent a strong likelihood that the transmitted bit was a '0' and larger positive values represent a strong likelihood that the transmitted bit was a '1'. This output is sent to a hard decision device to get the binary stream of data [6].

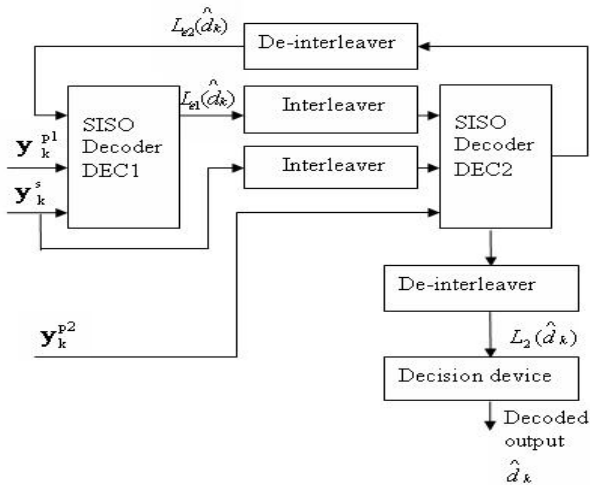


Figure 2. Turbo Decoder

C. Decoding Algorithms

Various algorithms are used for turbo decoding such as MAP algorithm, Log-MAP algorithm, Max-Log-MAP algorithm, Max-Log-MAP algorithm, Soft Output Viterbi Algorithm (SOVA). Turbo-code decoding requires a posteriori probability (APP) for each data bit. The data bit value corresponding to the maximum APP for that bit is chosen. The MAP algorithm splits the paths into two sets: those that have an information bit as '1' at step k and those that have a '0', returning the LLR of these two sets. The implementation of MAP algorithm is similar to performing Viterbi algorithm in two directions on code bits. MAP algorithm uses forward state

metric α_k^m at time k and state m , reverse state metric β_k^m at time k and state m , and a branch metric $\gamma_k^{i,m}$ at time k and state m [1],[3].

$$\Lambda(\hat{d}_k) = \frac{\sum_m \alpha_{k-1}^m \gamma_k^{1,m} \beta_k^{f(1,m)}}{\sum_m \alpha_{k-1}^m \gamma_k^{0,m} \beta_k^{f(0,m)}} \quad (1)$$

where $\Lambda(\hat{d}_k)$ is the likelihood ratio and $f(i, m)$ represents next state given (input, state) as (i, m) .

Logarithm of the likelihood ratio is the log-likelihood ratio (LLR) which is a real number representing soft decision output of a decoder. LLR of a systematic decoder is represented with three elements – a channel measurement $L_c(x)$, a priori knowledge of the data $L_a(d)$, and an extrinsic LLR $L_e(\hat{d})$. The extrinsic LLR is the extra knowledge gained from the decoding process.

$$L(\hat{d}) = L_c(x) + L_a(d) + L_e(\hat{d}) \quad (2)$$

In Max*-log-map algorithm, the Log-MAP algorithm is implemented based on *Jacobian algorithm* [7] as given below:

$$\ln(e^x + e^y) = \max(x, y) + \ln(1 + e^{-|x-y|}) \quad (3)$$

$$= \max(x, y) + f_c(|x - y|)$$

Max-Log-MAP algorithm reduces computational complexity of Log-MAP algorithm with a slightly poorer BER performance [8]. This algorithm looks at only two paths *per step*: the best with bit zero and the best with bit one at transition k , returning the difference of the log-likelihoods as LLR [8].

$$\ln \sum_j e^{a_j} \approx \max_j (a_j) \quad (4)$$

SOVA decoding works with the same metric as Max-Log-MAP algorithm, but the information returned about the reliability of decoded bit d_k is computed in a different way. The SOVA considers only one competing path per decoding step. That is to say, for each bit d_k , it considers only the survivor path of the Viterbi algorithm among all the competing paths. The MAP algorithm can outperform SOVA decoding by 0.5 dB or more[1].

III. SYSTEM MODEL

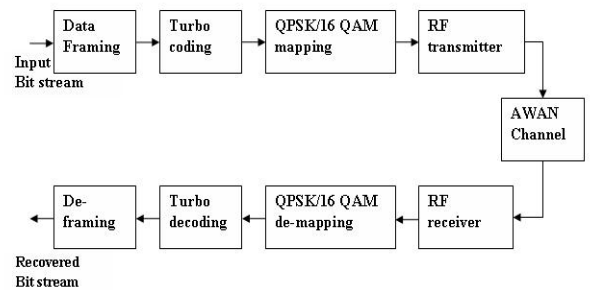


Figure 3. Turbo coded system

System model used in the simulation is shown in Fig. 3. The input bits are converted to frames and given as input to a rate $\frac{1}{3}$ PCCC turbo encoder. The generator used in the system is $G=[7,5]_8$. The encoded data stream is then modulated using QPSK/16-QAM as per gray coded constellation mapping. The complex symbols are passed on AWAN channel. At the receiver soft output de-mapping is used for QPSK/16-QAM demodulation along with appropriate channel values or LLRs for the turbo decoding. Max*-log-map algorithm is used in turbo decoding.

Simplified soft-output de-mapper used at the receiver reduces complexity of 16-QAM demodulation largely and improves the coding gain [9]. As per [9], if $b_1b_2b_3b_4$ are the bits representing 16-QAM constellation where b_1b_2 are mapped to the in-phase component and b_3b_4 are mapped to the quadrature component, then we estimate the soft de-mapped bits as given below:

$$\text{LLR}(b_i) = \ln \left(\frac{\sum_{b_i=+1} P(s_I(b_i)/x)}{\sum_{b_i=-1} P(s_I(b_i)/x)} \right) \text{ for } b_1b_2 \quad (5)$$

$$\text{LLR}(b_i) = \ln \left(\frac{\sum_{b_i=+1} P(s_Q(b_i)/x)}{\sum_{b_i=-1} P(s_Q(b_i)/x)} \right) \text{ for } b_3b_4$$

Gray mapped signal constellation of 16-QAM system is shown in fig.4. The corresponding input bits are marked in the order $b_1b_2b_3b_4$.

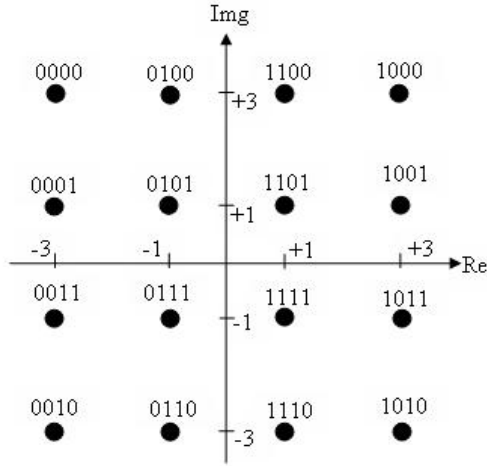


Figure 4. 16-QAM gray mapped constellation

Evaluation of the terms $D_{I,k}$ for the in-phase bits and $D_{Q,k}$ for the quadrature bits of a 16-QAM symbol yields[9]:

$$D_{I,1} = \begin{cases} y_I(i), & \text{for } |y_I(i)| \leq 2 \\ 2(y_I(i) - 1), & \text{for } y_I(i) > 2 \\ 2(y_I(i) + 1), & \text{for } y_I(i) < -2 \end{cases}$$

$$D_{I,2} = -|y_I(i)| + 2$$

$$D_{Q,1} = \begin{cases} -y_Q(i), & \text{for } |y_Q(i)| \leq 2 \\ -2(y_Q(i) - 1), & \text{for } y_Q(i) > 2 \\ -2(y_Q(i) + 1), & \text{for } y_Q(i) < -2 \end{cases} \quad (6)$$

$$D_{Q,2} = -|y_Q(i)| + 2$$

where $Y_I(i)$ and $Y_Q(i)$ are the real (in-phase) and imaginary (quadrature) components of the i^{th} received symbol propagated through AWGN channel. $D_{I,1}$, $D_{I,2}$, $D_{Q,1}$ and $D_{Q,2}$ represent the LLR values corresponding to b_1 through b_4 .

A. Turbo decoding Over AWAN Channel

As class A noise statistics is much different from additive white Gaussian noise (AWGN) channel, the conventional receivers which are optimized for AWGN channel are not suitable for AWAN channels.

Impulsive noise is one of the major problems in power line channel. Middleton's class A noise model defines the PDF with impulsive index A , Gaussian-to-impulsive noise power ratio Γ , Gaussian noise power σ_G^2 , and impulsive noise power σ_I^2 as follows [4],[10]:

$$p_A(x) = \sum_{m=0}^{\infty} \left(\frac{e^{-A} A^m}{m!} \right) \left(\frac{1}{\sqrt{2\pi\sigma_m^2}} \right) \exp \left(-\frac{x^2}{2\sigma_m^2} \right) \quad (7)$$

where $\sigma_m^2 = \frac{\sigma^2 \left(\frac{m}{A} + \Gamma \right)}{1 + \Gamma}$ and $\Gamma = \frac{\sigma_G^2}{\sigma_I^2}$. The total noise

power is given as $\sigma^2 = \sigma_G^2 + \sigma_I^2$. Sources of impulsive noise exhibit Poisson distribution $\frac{e^{-A} A^m}{m!}$

contributing to noise with Gaussian PDF and variance $\frac{\sigma_I^2}{A}$. At

a given time, assuming m such sources, the receiver noise exhibits Gaussian PDF with variance $\sigma_m^2 = \sigma_G^2 + \frac{m\sigma_I^2}{A}$.

For larger A , class a noise is approaching Gaussian noise.

In Turbo decoding, for an AWGN channel, the channel value is derived for BPSK (or QPSK) modulation as $L_c(y_k) = 4 \cdot \frac{E_s}{N_0} \cdot y_k$ (8)

where E_s is the energy per symbol and N_0 , the Gaussian noise power spectral density. This channel value is not suitable for AWAN channel.

With a correction in [10], the computation of the channel value $L_c(y_k)$ for turbo coded BPSK system is given below:

$$L_c(y_k) = \ln \left(\frac{P(y_k/u_k = +1)}{P(y_k/u_k = -1)} \right) = \ln \left(\frac{p_A(y_k - 1)}{p_A(y_k + 1)} \right) \quad (9)$$

$$= \ln \left(\frac{\sum_{m=0}^{\infty} \left(\frac{A^m}{m!} \right) \sqrt{\frac{A(1+\Gamma)}{m+A\Gamma}} \exp \left(-\frac{E_s}{N_0} \left(\frac{A\Gamma}{m+A\Gamma} \right) (y_k - 1)^2 \right)}{\sum_{m=0}^{\infty} \left(\frac{A^m}{m!} \right) \sqrt{\frac{A(1+\Gamma)}{m+A\Gamma}} \exp \left(-\frac{E_s}{N_0} \left(\frac{A\Gamma}{m+A\Gamma} \right) (y_k + 1)^2 \right)} \right)$$

where $\frac{E_s}{N_0} = \frac{1}{2\sigma^2}$. If $\Gamma \ll 1$, then (9) reduces to

$$L_c(y_k) = \ln \left(\frac{\sum_{m=0}^{\infty} \left(\frac{A^m}{m!} \right) \sqrt{\frac{A\Gamma}{m+A\Gamma}} \exp\left(-\frac{E_s}{N_0} \left(\frac{A\Gamma}{m+A\Gamma} \right) (y_k - 1)^2\right)}{\sum_{m=0}^{\infty} \left(\frac{A^m}{m!} \right) \sqrt{\frac{A\Gamma}{m+A\Gamma}} \exp\left(-\frac{E_s}{N_0} \left(\frac{A\Gamma}{m+A\Gamma} \right) (y_k + 1)^2\right)} \right) \quad (10)$$

For turbo coded QPSK system, $L_c(k)$ computation remains same except that y_k in (10) is replaced by $y_l(k)$ for LLR of first bit of QPSK mapping and $y_Q(k)$ for the second bit.

For a 16-QAM system with constellation as in Fig.4, the likelihood functions with AWGN noise model are given below:

$$\begin{aligned} \frac{p(y/b_1=1)}{p(y/b_1=0)} &= \frac{\exp(-(y_l-1)^2/(2\sigma^2)) + \exp(-(y_l-3)^2/(2\sigma^2))}{\exp(-(y_l+1)^2/(2\sigma^2)) + \exp(-(y_l+3)^2/(2\sigma^2))} \\ \frac{p(y/b_2=1)}{p(y/b_2=0)} &= \frac{\exp(-(y_l-1)^2/(2\sigma^2)) + \exp(-(y_l+1)^2/(2\sigma^2))}{\exp(-(y_l-3)^2/(2\sigma^2)) + \exp(-(y_l+3)^2/(2\sigma^2))} \end{aligned}$$

and

$$\begin{aligned} \frac{p(y/b_3=1)}{p(y/b_3=0)} &= \frac{\exp(-(y_Q+1)^2/(2\sigma^2)) + \exp(-(y_Q+3)^2/(2\sigma^2))}{\exp(-(y_Q-1)^2/(2\sigma^2)) + \exp(-(y_Q-3)^2/(2\sigma^2))} \\ \frac{p(y/b_4=1)}{p(y/b_4=0)} &= \frac{\exp(-(y_Q-1)^2/(2\sigma^2)) + \exp(-(y_Q+1)^2/(2\sigma^2))}{\exp(-(y_Q-3)^2/(2\sigma^2)) + \exp(-(y_Q+3)^2/(2\sigma^2))} \end{aligned} \quad (11)$$

where y is the received symbol at that instant.

The LLR of four bits of a given symbol are computed in the proposed model using (7), (9) and (11). Let $L_c(y_{k,i})$ represent the LLR of i^{th} bit of the k^{th} received QAM symbol where $i=1,2,3,4$ in the 16-QAM system. Also, let $y_{l,k}$ and $y_{Q,k}$ represent the real and the imaginary parts of received symbol y_k respectively.

$$L_c(y_{k,1}) = \ln \left(\frac{\sum_{m=0}^{\infty} \left(\frac{A^m}{m!} \right) \sqrt{\frac{A\Gamma}{m+A\Gamma}} (num)}{\sum_{m=0}^{\infty} \left(\frac{A^m}{m!} \right) \sqrt{\frac{A\Gamma}{m+A\Gamma}} (den)} \right)$$

where

$$\begin{aligned} num &= \exp\left(-\frac{E_s}{N_0} \left(\frac{A\Gamma}{m+A\Gamma} \right) (y_{l,k} - 1)^2\right) + \exp\left(-\frac{E_s}{N_0} \left(\frac{A\Gamma}{m+A\Gamma} \right) (y_{l,k} - 3)^2\right) \\ den &= \exp\left(-\frac{E_s}{N_0} \left(\frac{A\Gamma}{m+A\Gamma} \right) (y_{l,k} + 1)^2\right) + \exp\left(-\frac{E_s}{N_0} \left(\frac{A\Gamma}{m+A\Gamma} \right) (y_{l,k} + 3)^2\right) \end{aligned} \quad (12)$$

LLR computation for first bit, i.e. b_1 of the k^{th} received symbol is given in (12). Similarly, LLR for the other three bits of the k^{th} symbol can be computed. Computation complexity can be reduced as per the description in [10].

IV. NUMERICAL RESULTS

The results obtained by MATLAB simulations are given in terms of BER versus E_b/N_0 , where E_b is the energy per information bit. The performance of rate $1/3$ Turbo coded system over AWAN channel is verified for two possible modulation formats, QPSK and 16-QAM. Data frame size of 2000 is used and 500 such frames are considered in the simulation. We consider impulsive index $A=0.1$ and Gaussian to impulsive noise ratio (GIR) $\Gamma=0.1$ for the AWAN channel. For turbo decoding, results of 9th iteration are considered.

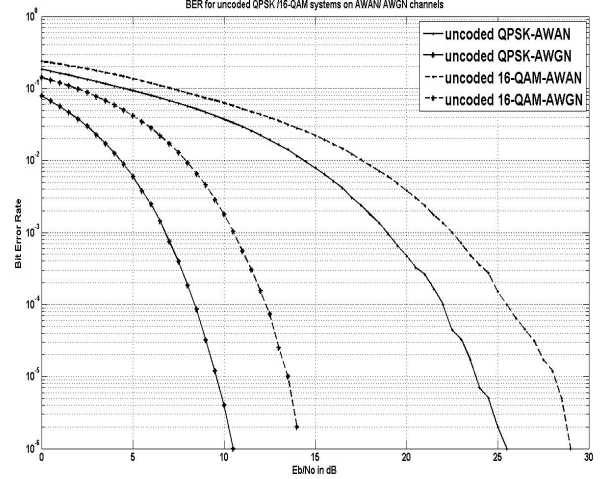


Figure 5. Uncoded QPSK/16-QAM system on AWGN/AWAN channel

In Fig. 5, we show the performance of uncoded QPSK/16-QAM system on AWGN as well as AWAN channels. We note that the uncoded QPSK/16-QAM system on AWAN channel exhibits very much poor BER performance as compared to the same on AWGN channel. At a BER = 10^{-5} , the deviation of the AWAN system is 14 dB as compared to AWGN channel response. It is 14.7 dB for 16-QAM system.

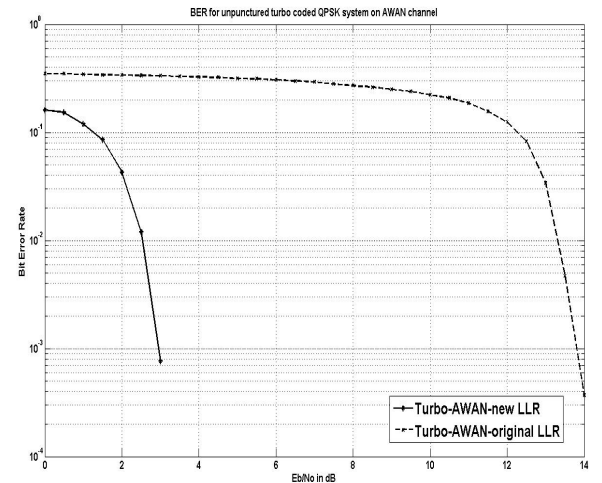


Figure 6. Turbo coded QPSK system on AWAN channel

In Fig.6, we compare the performance of Turbo coded QPSK system on AWAN channel for two different LLRs. We compute the channel value as per two conditions – one with AWGN scenario and the other with AWAN. Observation plots are given for system with these LLR computations. At a BER = 10^{-3} , the performance improvement of system with channel value computed as per AWAN channel conditions is around 10.9 dB compared to system with channel value computed as per AWGN channel conditions.

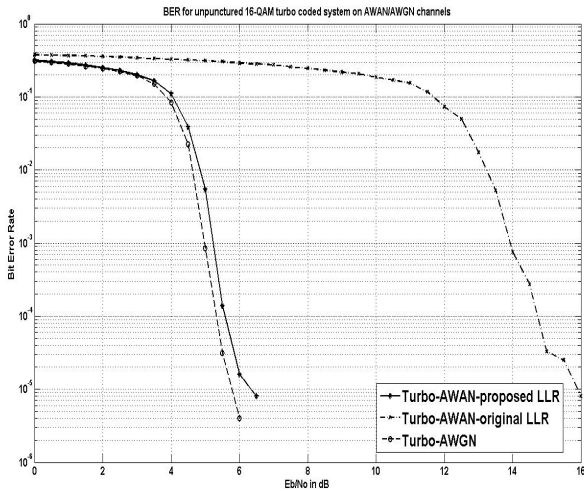


Figure 7. Turbo coded 16-QAM system on AWAN/AWGN channels

In Fig. 7, performance comparison of un-coded 16-QAM system on AWGN channel with Turbo coded 16-QAM system on AWAN channel with different channel values for the turbo decoder is given. Response of 16-QAM system on AWGN channel is also plotted. We observe that at a BER = 10^{-5} , the performance improvement of the system with channel value computed as per AWAN channel conditions is around 9.6 dB compared to system with channel value computed as per AWGN channel conditions. Also, the deviation of AWAN response from AWGN response at a BER = 10^{-5} is only 0.5 dB.

V. CONCLUSIONS

We have discussed Turbo decoding over AWAN channels for Turbo coded QPSK/ 16-QAM systems in this paper. It is shown that class A noise can be effectively filtered out with this model. Turbo coded QPSK system with proposed LLR as compared to original LLR, gives performance improvement by around 11 dB at a BER of 10^{-3} . Similarly, Turbo coded 16-QAM system with proposed LLR as compared to original LLR, gives performance improvement by around 10 dB at a BER of 10^{-5} . We have also shown that BER performance of the proposed model is very close to that of AWGN channel. Hence we conclude that the proposed model is suitable for class A noise filtering at the receiver.

REFERENCES

- [1] Bernard Sklar, "Digital communications- Fundamentals and applications," 2nd ed., Pearson Education (Singapore) Pte. Ltd, 2004, pp. 477-511.
- [2] Ahmad R.S. Bahai, Burton R. Saltzberg, Mustafa Ergen, "Multi-carrier digital communications-theory and applications of OFDM", 2nd ed., Springer Science and business media, Inc., pp. 5-14 and 27-53, 2004
- [3] Berrou C, Glavieux A and Thitimajshima P, "Near Shannon Limit Error-Correcting Coding and Decoding : Turbo Codes", *IEEE proc. of the Int. Conf. on communications*, pp. 1064-1070, May 1993
- [4] D. Middleton, "Statistical-physical model of electromagnetic interference," *IEEE Trans. Electromagn. Compat.*, vol. EMC-19, no. 3, pp. 106-126, Aug. 1977
- [5] E. Biglieri and P. de Torino, "Coding and modulation for a horrible channel," *IEEE Commun. Mag.*, vol. 41, no. 5, pp. 92-98, May 2003
- [6] Savitha H. M. and Muralidhar Kulkarni, "Performance Comparison of Hard and Soft-decision Turbo Coded OFDM Systems", to be published in *IEEE proc. of WCNIS 2010*
- [7] Patrick Robertson, Emmanuelle Villebrun and Peter Hoeher, "A comparison of optimal and sub-optimal MAP decoding algorithms operating in the log domain", *IEEE Int. Conf. on Communications*, vol.2, pp. 1009-1013, June 1995
- [8] W.J. Gross and P.G. Gulak, "Simplified MAP algorithm suitable for implementation of turbo decoders," *Electronics Letters*, Vol. 34, pp. 1577-1578, Aug. 1998
- [9] Filippo Tosato, Paola Bisaglia, "Simplified soft-output demapper for Binary Interleaved COFDM with application to HIPERLAN/2," *IEEE Int. Conf. on Communications*, vol.2, pp. 664- 668, Aug. 2002
- [10] D. Umehara, H. Yamaguchi, and Y. Morihoro, "Turbo Decoding in Impulsive Noise Environment", *IEEE Globecom 2004*, pp. 194-198, Nov 2004